Struct Multidisc Optim (2017) 56:331–351
DOI 10.1007/s00158-017-1667-7

RESEARCH PAPER

An efficient method for reliability-based design optimization of nonlinear inelastic steel space frames

V. H. Truong[1] · **Seung-Eock Kim**[1]

Received: 4 September 2016 / Revised: 13 January 2017 / Accepted: 3 February 2017 / Published online: 14 March 2017

Abstract This paper proposes an effective numerical procedure for reliability-based design optimization (RBDO) of nonlinear inelastic steel frames by integrating a harmony search technique (HS) for optimization and a robust method for failure probability analysis. The practical advanced analysis using the beam-column approach is used for capturing the nonlinear inelastic behaviors of frames, while a detail implement of HS for discrete optimization of steel frames is introduced. The failure probability of structures is evaluated by using the combination of the improved Latin Hypercube (IHS) and a new effective importance sampling (EIS). The efficiency and accuracy of the proposed procedure are demonstrated through three mathematical examples and five steel frames. The results obtained in this paper prove that the proposed procedure is computationally efficient and can be applied in practical design. Furthermore, it is shown that the use of nonlinear inelastic analysis in the optimization of steel frames yields more realistic results.

Keywords Reliability-based optimization · Steel frame · Advanced analysis · Harmony search · Reliability analysis · Latin hypercube · Importance sampling

✉ Seung-Eock Kim
sekim@sejong.ac.kr

V. H. Truong
truongviethung82@sju.ac.kr

[1] Department of Civil and Environmental Engineering, Sejong University, 98 Gunja Dong, Gwangjin Gu Seoul 143-747, South Korea

1 Introduction

The optimization of steel frames has been attracting the interest of many researchers in recent years since this approach reduces costs and guarantees performance of structures. In optimization, the frame weight is minimized by selecting the lightest cross-sectional area from the standard lists of sections (e.g. AISC, Eurocode, etc.), while the performance requirements are still satisfied. The optimization of steel frames is hence a discrete optimization and requires metaheuristic algorithms for solving discrete variable spaces. Based on considering or ignoring probabilistic constraints, the optimization of steel frames is divided into deterministic design optimization (DDO) and reliability-based design optimization (RBDO), respectively.

Many researches concerning DDO of steel frames have been carried out in the literature with various algorithms and techniques being proposed (Hasançebi et al. 2009, 2010a, b; Kripakaran et al. 2011; Doğan and Saka 2012; Alberdi and Khandelwal 2015). In these researches, considerable effort has been used to improve and develop metaheuristic optimization algorithms since these techniques are accepted as the standard design optimization tools for the foreseeable future (Saka and Geem 2013). Some of the well-known metaheuristic optimization algorithms are ant colony optimization (ACO) (Camp et al. 2005), genetic algorithm (GA) (Rajeev and Krishnamoorthy 1992), harmony search (HS) (Lee and Geem 2004), particle swarm optimization (PSO) (Perez and Behdinan 2007), simulated annealing (SA) (Balling 1991), Tabu search (TS) (Bland 1995), etc. The review of metaheuristic algorithms for steel frames is presented by Saka and Geem (2013). Although there has been significant improvement in the study of metaheuristic algorithms, most of their applications are limited to linear frames where the member-based design method is used for evaluating strength

and inter-story drift constraints. The member-based design method in conventional design codes is unattractive since the capacity of individual members is checked using the effective length factor instead of considering the interaction of stability and strength between the member and whole frame. Therefore, there have been significant efforts for developing practical advanced analyses (PAAs) which can capture the nonlinear inelastic behaviors and eliminate the individual member check of a whole frame (Clarke 1994; Teh and Clarke 1999; Chen and Kim 1997; Kim and Chen 1996; Tai and Kim 2009). In addition, the DDO of nonlinear steel frames has been attracting the interest of researchers in recent years (Saka and Kameshki 1998; Kameshki and Saka 2003; Degertekin 2007; Degertekin and Hayaliolu 2010; Truong et al. 2017). The results in these works showed that the lighter and realistic optimum designs were obtained when considering structural nonlinear behaviors in optimization.

Although there have been many researches concerning DDO of steel frames, few studies related to RBDO of steel frames have been carried out. Among these studies, an RBDO procedure for nonlinear large-scale frames is proposed by Tsompanakis and Papadrakakis (2004) using evolution strategies (ES) for optimization and importance sampling technique (IS) for reliability analysis. However, the case studies do not take the different probabilistic distributions of applied loads into account. Furthermore, the capacities of IS are significantly decreased when the number of random variables increases. A combination of decoupling for optimization and the metamodel for reliability analysis is proposed by Valdebenito and Schuëller (2010) in terms of GA, IS, and Subset simulation (SS) techniques to investigate the RBDO optimum solution of frames. This method seems very robust since the computational cost is low, but only local optimum solutions are found. In addition, geometric and material nonlinear behaviors are not considered. An RBDO procedure of structures is developed by Shayanfar et al. (2014) using GA for optimization, first-order reliability method (FORM) for reliability analysis, and OpenSees and Tcl for structural analysis. This procedure is not reliable since only linear analysis of frames is considered and the error of FORM in a highly nonlinear system is quite large.

In the present work, a robust procedure for RBDO of space steel frames is proposed. The objective of optimization is to minimize the total weight of the frame, while the constraints are both deterministic (stress, displacement, and geometric constructional limitations) and probabilistic (the overall failure probability of the structure) constraints. The contribution of this work is as follows: the nonlinear inelastic behaviors of frames are predicted by using the beam-column approach; a detailed implementation of HS for discrete optimization of steel frames is introduced; and, an efficient reliability analysis method (IHS-EIS) is proposed. IHS-EIS is the combination of the improved Latin Hypercube Sampling (IHS) proposed by Beachkofski and Grandhi (2002) and a new effective importance sampling (EIS). Three mathematical examples and five steel frames are considered to demonstrate the efficiency and accuracy of the propose procedure.

2 Reliability-based design optimization of steel frames

In this study, the RBDO of steel frames is formulated for achieving the minimization of total structural weight subjected to deterministic and probabilistic constraints. Deterministic constraints are limits on member stresses, nodal displacements or inter-story drifts, and geometric constructability. The probabilistic constraint ensures the condition that the overall failure probability of frame is smaller than a certain value (e.g. 10^{-3}).

2.1 Objective function

The objective function of the RBDO of steel frames can be expressed as follows:

$$Min \quad W(Y,X) = \rho \sum_{i=1}^{n} \left(A(y_i) \sum_{q=1}^{n_q} L_q \right), \tag{1}$$

where ρ is the specific weight of steel; n and $Y=(y_1, y_2, \ldots, y_n)$ are the number and vector of design variables, respectively; $X=(x_1, x_2, \ldots, x_m)$ is the vector of random variables; n_q is the number of frame member groups; L_q is the length of the member q in the group i^{th}; and, $A(y_i)$ is the cross-sectional area of the design variable y_i. $A(y_i)$ is selected from the list of W-shaped sections given by AISC-LRFD specification (1999). Furthermore, according to AISC-LRFD, the response of the structure to service loads generally can be analyzed by assuming elastic behavior.

2.2 Deterministic constraints

The constraint of member stresses considering PAA can be expressed on the condition that the structural load-carrying capacity R is larger than the applied load S as follows:

$$C^{str} = 1 - \frac{R}{S} \le 0. \tag{2}$$

The inner-story drift constraints can be expressed as follows:

$$C_j^{ins} = \frac{|d_j|}{|d_j^u|} - 1 \le 0 \quad j = 1, \ldots, n_{story}, \tag{3}$$

where n_{story} is the number of structural stories; d_j and d_j^u are the inter-story displacement and allowable inter-story displacement of the story j, respectively.

Geometric constructional constraints are formulated as follows:

$$C_{k,1}^{con} = \left(\frac{b_{bf}}{b_{cf}}\right)_k - 1 \le 0, \tag{4.a}$$

$$C_{k,2}^{con} = \left(\frac{b_{bf2}}{T_c}\right)_k - 1 \le 0, \tag{4.b}$$

where $k = 1, \ldots, n_{con}$; n_{con} is the number of geometric constructional constraint; T_c is the web height of column; and, b_{bf}, b_{bf2}, and b_{cf} are the flange width of beam and column as given in Fig. 1.

2.3 Probabilistic constraint

The probabilistic constraint (the condition that the overall failure probability of the structure is smaller than a certain value) can be expressed as

$$C^{prob} = \frac{P_f(X)}{P_a} - 1 \le 0, \tag{5}$$

where $P_f(X)$ and P_a are the failure probability and the allowable failure probability, respectively.

2.4 Unconstrained objective function

The constrained objective function in (1) can be transformed to unconstrained objective function by adding a penalty function as follows:

$$W(Y) = \rho \sum_{i=1}^{n} \left(A(y_i) \sum_{q=1}^{n_q} L_q \right) \times \left(\alpha_{str}\beta_1 + \alpha_{inn}\beta_2 + \alpha_{con}\beta_3 + \alpha_{prob}\beta_4 \right), \tag{6}$$

where

$$\begin{aligned} \beta_1 &= \max(C^{str}, 0) \\ \beta_2 &= \sum_{j=1}^{n_{story}} \max\left(C_j^{ins}, 0\right) \\ \beta_3 &= \sum_{k=1}^{n_{con}} \left(\max\left(C_{k,1}^{con}, 0\right) + \max\left(C_{k,2}^{con}, 0\right) \right) \\ \beta_4 &= \max\left(C^{prob}, 0\right) \end{aligned}, \tag{7}$$

in which α_{str}, α_{inn}, α_{con}, and α_{prob} are penalty factors corresponding to the violation of strength, inner-story drift, constructability, and failure probability of structure, respectively.

RBDO of steel frames presented in (7) is a discrete optimization problem, in which the cross-sectional areas of frame members are selected from a list of W-shaped sections. Therefore, metaheuristic methods are often employed to solve this problem. Among the well-known metaheuristic methods, *HS* is used in this study because this algorithm is quite efficient for frame optimization (Alberdi and Khandelwal 2015). In addition, PAA using the beam-column approach is employed to capture nonlinear inelastic behaviors of steel frames and the Monte Carlo simulation (MCS) based method is applied to evaluate the probability constraint, since most steel frames are highly nonlinear structures.

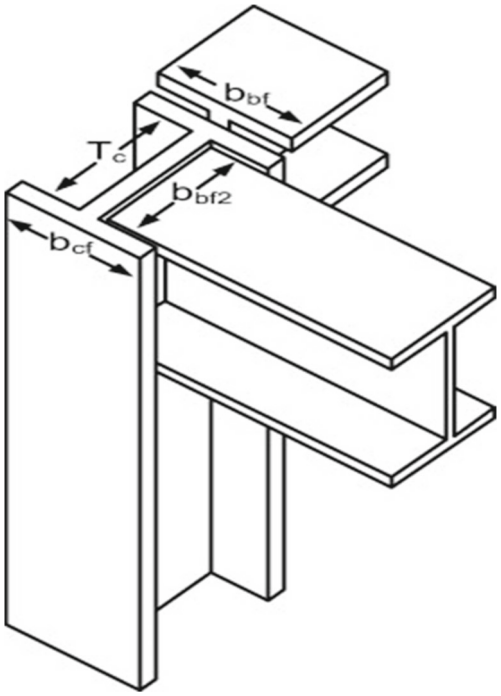

Fig. 1 Beam to column connection constructability

3 PAA of space steel frames

Most PAA methods for analysis of nonlinear inelastic steel frames presented in literature can be classified into plastic zone methods (Clarke 1994; Teh and Clarke 1999) and plastic hinge methods (Chen and Kim 1997; Kim and Chen 1996; Thai and Kim 2009). In plastic zone methods, interpolation functions are adopted to represent the second-order effects while plastic zone models are used to capture the spread of nonlinear behavior along the structural elements. Although designated as 'exact' methods, these methods have not been widely applied to the actual design due to their excessive computational time. In the plastic hinge method or beam-column approach, stability functions derived from differential equilibrium equations are used to capture second-order effects of frames. The refined plastic hinge model is also adopted to account for nonlinear inelastic behaviors of frames. The advantage of this method is that one or two elements are needed to model a frame member, so the computational time decreases considerably. As a consequence, the beam-column approach is employed in this study.

3.1 Beam-column element

In a beam-column element, the stability functions proposed by Chen and Lui (1987) is employed to capture P-δ effect, while the column research council (CRC) tangent modulus concept (Chen and Lui 1992) is used to account for initial geometric imperfection and residual stresses. The gradual stiffness degradation model using Orbison yield surface (Orbison et al. 1982) is also employed to consider the case of small axial force and large bending moments. The force-displacement relationship of the element AB is written as:

$$\begin{Bmatrix} \Delta P \\ \Delta M_{yA} \\ \Delta M_{yB} \\ \Delta M_{zA} \\ \Delta M_{zB} \\ \Delta T \end{Bmatrix} = \begin{bmatrix} E_t A/L & 0 & 0 & 0 & 0 & 0 \\ 0 & k_{iiy} & k_{ijy} & 0 & 0 & 0 \\ 0 & k_{ijy} & k_{jjy} & 0 & 0 & 0 \\ 0 & 0 & 0 & k_{iiz} & k_{ijz} & 0 \\ 0 & 0 & 0 & k_{ijz} & k_{jjz} & 0 \\ 0 & 0 & 0 & 0 & 0 & GJ/L \end{bmatrix} \begin{Bmatrix} \Delta\delta \\ \Delta\theta_{yA} \\ \Delta\theta_{yB} \\ \Delta\theta_{zA} \\ \Delta\theta_{zB} \\ \Delta\phi \end{Bmatrix}, \quad (8)$$

in which E_t and G are the reduced-elastic and shear modulus of material, respectively; L and A are the length and area of the element, respectively; J is the torsional constant; ΔP and ΔT are the incremental axial force and incremental torsional moment, respectively; ΔM_{nN} is the incremental moment at end N ($N = A, B$) according to axis n ($n = y, z$) of the element; $\Delta\delta$ and $\Delta\phi$ are the incremental axial displacement and incremental twist angle, respectively; $\Delta\theta_{nN}$ is the joint incremental rotation at end N of the element corresponding to axis n; and,

$$k_{iin} = \eta_A \left(S_{1n} - \frac{S_{2n}^2}{S_{1n}} (1-\eta_B) \right) \frac{E_t I_n}{L}, \quad (9.a)$$

$$k_{ijn} = \eta_A \eta_B S_{2n} \frac{E_t I_n}{L}, \quad (9.b)$$

$$k_{jjn} = \eta_B \left(S_{1n} - \frac{S_{2n}^2}{S_{1n}} (1-\eta_A) \right) \frac{E_t I_n}{L}, \quad (9.c)$$

where I_n, S_{1n} and S_{2n} are the inertia moment and stability functions corresponding to axis n, respectively; η_A and η_B are scalar parameters representing the gradual inelastic stiffness reduction of the element due to plastification at A and B, respectively. η can be determined by using the Orbison yield surface parameter α as follows:

$$\eta = 1.0 \; for \; \alpha \le 0.5, \quad (10.a)$$

$$\eta = 4\alpha(1-\alpha) \; for \; \alpha > 0.5, \quad (10.b)$$

$$\text{with} \quad \alpha = 1.15p^2 + m^2 + 3.67p^2m^2, \quad p = P/P_y, \text{ and } \quad m = M/M_p. \quad (11)$$

To consider the influence of initial geometric imperfection and residual stresses, E_t in (8) can be calculated as

$$E_t = E \; for \; {}^{P}/_{P_y} \le 0.5, \quad (12.a)$$

$$E_t = 4\frac{P}{P_y} E \left(1 - \frac{P}{P_y} \right) \; for \; {}^{P}/_{P_y} > 0.5, \quad (12.b)$$

in which P_y is the axial yield force.

3.2 Nonlinear solution procedure

In order to solve the nonlinear equations, the generalized displacement control method (GDC) (Yang and Shieh 1990) is employed here since it is robust for nonlinear problems with multiple critical points. In GDC, the equilibrium equation of the iteration j^{th} in the incremental step i^{th} is written as follows:

$$\left[K_{j-1}^i\right] \left\{\Delta D_j^i\right\} = \lambda_j^i \left\{\hat{P}\right\} + \left\{R_{j-1}^i\right\}, \quad (13)$$

and can be decomposed as

$$\left[K_{j-1}^i\right] \left\{\Delta \hat{D}_j^{\,i}\right\} = \left\{\hat{P}\right\} \quad (14.a)$$

$$\left[K_{j-1}^i\right] \left\{\Delta \overline{D}_j^{\,i}\right\} = \left\{R_{j-1}^i\right\} \quad (14.b)$$

$$\left\{\Delta D_j^i\right\} = \lambda_j^i \left\{\Delta \hat{D}_j^{\,i}\right\} + \left\{\Delta \overline{D}_j^{\,i}\right\} \quad (14.c)$$

in which $[K_{j-1}^i]$ is the tangent stiffness matrix; $\{\Delta D_j^i\}$ is the displacement incremental vector; $\{\hat{P}\}$ and $\{R_{j-1}^i\}$ are the reference load and unbalanced force vectors, respectively; $\{\Delta \hat{D}_j^{\,i}\}$ and $\{\Delta \overline{D}_j^{\,i}\}$ are the displacement incremental vectors generated by the $\{\hat{P}\}$ and $\{R_{j-1}^i\}$, respectively; and, λ_j^i is the load incremental parameter.

In (13), λ_j^i is determined using a constraint condition as following steps:

- At the first iterative step ($j = 1$), λ_j^i is calculated as

$$\lambda_1^i = \lambda_1^1 \sqrt{|GSP|}, \quad (15)$$

where λ_1^1 is the initial value of the load increment parameter and GSP is the generalized stiffness parameter which is calculated as

$$GSP = \frac{\left\{\Delta \hat{D}_1^{\,1}\right\}^T \left\{\Delta \hat{D}_1^{\,1}\right\}}{\left\{\Delta \hat{D}_1^{\,i-1}\right\}^T \left\{\Delta \hat{D}_1^{\,i}\right\}}. \quad (16)$$

- At the iterative steps ($j \ge 2$), λ_j^i is calculated as

$$\lambda_j^i = -\frac{\left\{\Delta \hat{D}_1^{\,i-1}\right\}^T \left\{\Delta \overline{D}_j^{\,i}\right\}}{\left\{\Delta \hat{D}_1^{\,i-1}\right\}^T \left\{\Delta \hat{D}_j^{\,i}\right\}}. \quad (17)$$

The load factor Λ_j^i of the iteration j^{th} in the incremental step i^{th} can be calculated as

$$\Lambda_j^i = \Lambda_{j-1}^i + \lambda_j^i. \quad (18)$$

The total applied load vector $\{P_j^i\}$ and the total displacement vector $\{D_j^i\}$ of the structure at the iteration j^{th} in the incremental step i^{th} are determined as follows:

$$\left\{P_j^i\right\} = \Lambda_j^i\left\{\hat{P}\right\}, \tag{19.a}$$

$$\left\{D_j^i\right\} = \left\{D_{j-1}^i\right\} + \left\{\Delta D_j^i\right\}. \tag{19.b}$$

The procedure for nonlinear inelastic analysis is presented in Fig. 2.

4 Failure probability analysis of space steel frames

The limit state function of structure can be written as follows:

$$G(R,S) = R - S, \tag{20}$$

where R and S are the structural load-carrying capacity and the loading effect, respectively.

The structural failure probability is calculated as follows:

$$P_f = P[G(R,S) \le 0] = \int_{G(R,S)\le 0} f_R(r) f_S(s) dr ds, \tag{21}$$

in which $f_R(r)$ and $f_S(s)$ are the probability density functions of R and S, respectively.

In highly nonlinear frames, R cannot be determined analytically. Therefore, the integral of (21) is often estimated by approximate methods. Among the well-known approximate methods, MCS seems superior. However, MCS requires a very large number of samples when P_f is small. To overcome this limitation, IHS-EIS is developed herein by integrating IHS and EIS.

4.1 Improved Latin hypercube sampling

Latin Hypercube Sampling (LHS) is a stratified sampling technique which allows the effective sample creation to represent the distribution of a random variable. Many improvements of LHS have been proposed for multivariate variable problems (Beachkofski and Grandhi 2002; Tang 1998; Morris and Mitchell 1995; Owen 1994; Ye et al. 2000). Among these techniques, IHS proposed by Beachkofski and Grandhi (2002) is used in this study since it is robust and easy to implement.

The basis of IHS originates from the maximum of the minimum distance between sample points which is determined as follows:

$$d_{opt} = {}^{N}\Big/_{\sqrt[m]{N}}, \tag{22}$$

where N and m are the number of samples and random variables, respectively. The first sample point is randomly selected, while the next points are created by using the "piecewise deterministic optimization" technique. In this technique, a subspace is firstly developed by repeating l times of remaining available possibilities of variables. The point in the subspace, which having the value of minimum distance to the selected sample points closest to d_{opt}, is then selected. The value of l can be chosen from 5 to 10 (Beachkofski and Grandhi 2002).

4.2 Effective importance sampling method

Equation (14) can be rewritten as following for the general case:

$$P_f = \int_{G(X)\le 0} f_X(X) dX, \tag{23}$$

in which $X=(x_1, x_2, \ldots, x_m)$ is the vector of random variables and $f_X(X)$ is the joint probability. The IS technique is applied by rewriting (23) as follows:

$$P_f = \int_{G(X)\le 0} \frac{f_X(X)}{g_X(X)} g_X(X) dX, \tag{24}$$

where $g_X(X)$ is the IS distribution function. By applying the law of large numbers, the failure probability of structure is estimated as

$$P_f^{IS} \simeq \frac{1}{N}\sum_{i=1}^{N} I(X_i), \tag{25}$$

in which:

$$I(X_i) = \begin{cases} \dfrac{f_X(X_i)}{g_X(X_i)} & if\ G \le 0 \\ 0 & if\ G > 0 \end{cases}. \tag{26}$$

In PAA of a nonlinear system, $G(X)$ cannot be presented as a mathematical function, while the choice of $g_X(X)$ is very difficult due to the variety of the distribution of random variables. To overcome these limitations, EIS is proposed herein based on a new equation of $G(X)$ which allows the easy and automatic selection of IS function in numerical procedure. Moreover, compared to the IS, the variance of the structural failure probability using EIS is considerably decreased.

In order to develop a new equation of $G(X)$, Fig. 3 presents two safety check methods of a plane frame subjected to two applied loads (H, P). In the first method in Fig. 3a, the load factor lf, which is defined as the ratio of the ultimate load at the frame collapse to the applied load, is calculated by using PAA. The frame is safe if lf is larger than 1.0. In the second method as shown in Fig. 3b, the frame deformation due to P is firstly captured, and the load-carrying capacity R_H of the frame in

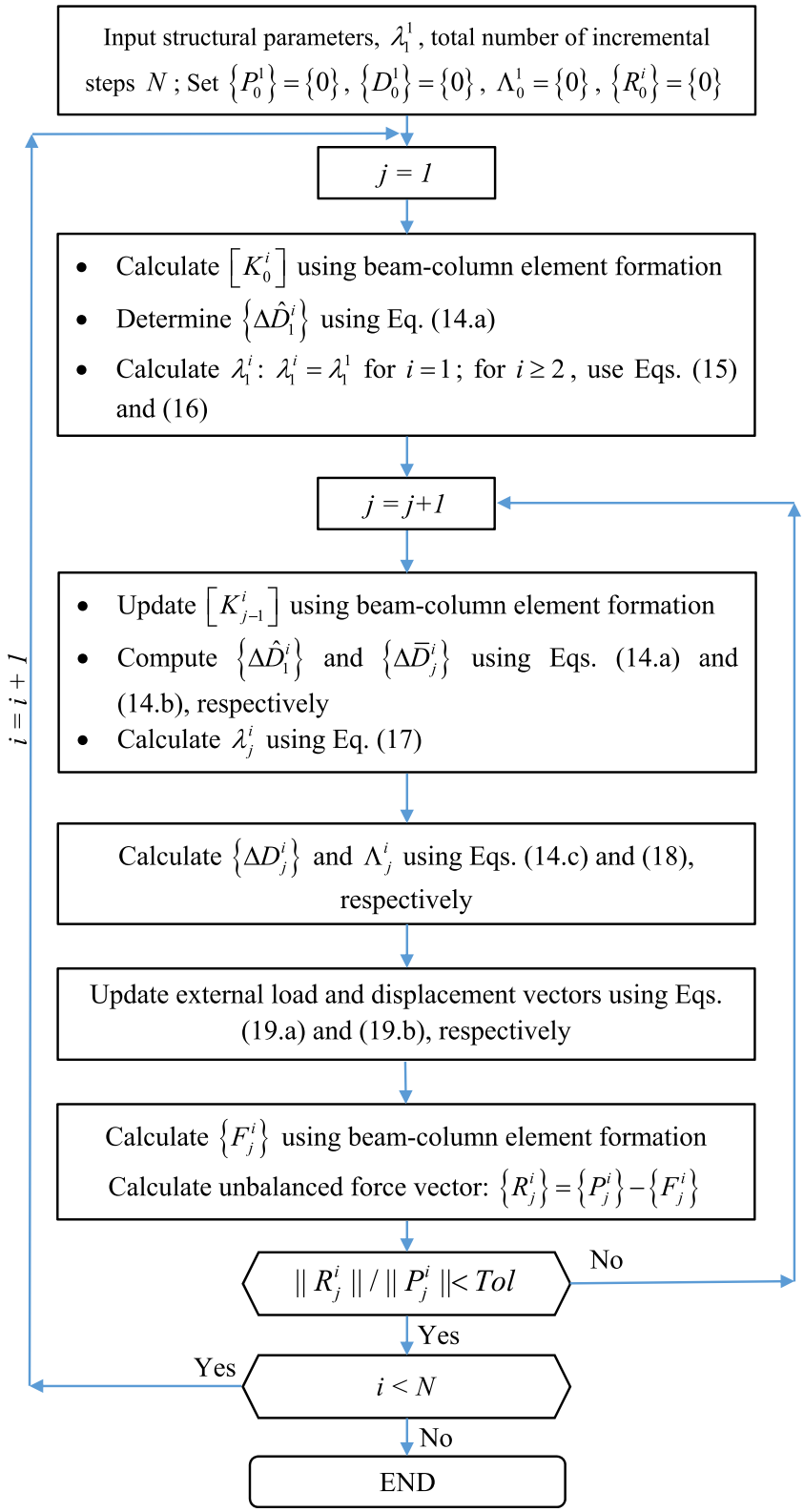

Fig. 2 Flow-chart of nonlinear inelastic analysis

terms of H is then calculated. The frame safety condition in this case is that R_H must be larger than H.

Now, consider the case that the value of H is changed while the value of P is preserved. To check the frame safety, the second method requires only one structural analysis while the first method needs the number of structural analyses equal to the number of values of H. Hence from the simulation view point, the second method is much better than the first method.

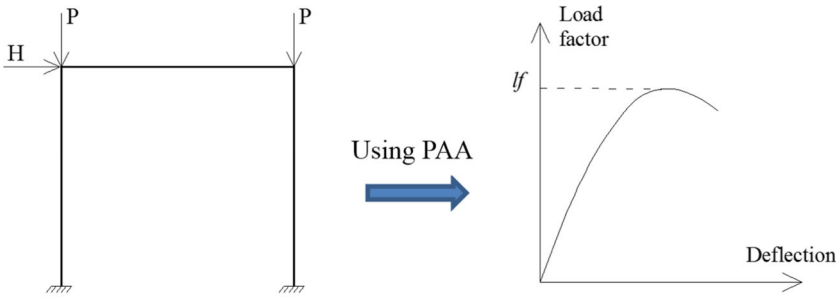

(a) Method 1

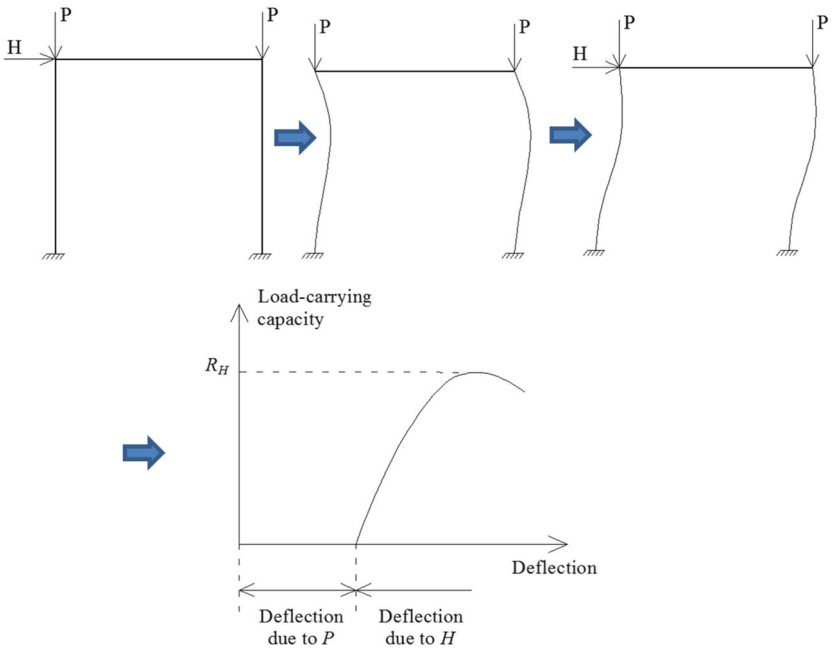

(b) Method 2

Fig. 3 Methods of safety checking of simple planar frame. **a** Method 1. **b** Method 2

The limit state function of the frame using the second method can be written as

$$G(H,P) = R_H - H. \tag{27}$$

In the general case, (27) can be rewritten as

$$G(X) = R_{xm}(x_1, x_2, \ldots, x_{m-1}) - x_m, \tag{28}$$

where $X = (x_1, x_2, \ldots, x_m)$ is the vector of random variables; x_m is an applied load; and, R_{xm} is the structural load-carrying capacity in terms of x_m.

The structural failure probability is calculated as follows:

$$P_f = P[G(X) \le 0] = \int_{G(X)\le 0} f_{R_{xm}}(r) f_{x_m}(x)\, dr dx, \tag{29}$$

where $f_{R_{xm}}(r)$ and $f_{x_m}(x)$ are probability functions of R_{xm} and x_m, respectively.

To apply the IS technique, (29) is rewritten as follows:

$$P_f = P[G(X) \le 0] = \int_{G(X)\le 0} f_{R_{xm}}(r) g_{x_m}(x) \frac{f_{x_m}(x)}{g_{x_m}(x)} dr dx, \tag{30}$$

where $g_{x_m}(x)$ is the IS distribution function of x_m.

The failure probability of structure according to the IS method can be calculated as:

$$P_f^{IS} \simeq \frac{1}{N} \sum_{i=1}^{N} I\left(x_m{}^i\right), \tag{31}$$

where N is the number of samples; x_m^i is the sample i^{th} of x_m by using $g_{x_m}(x)$; and, $I(x_m^i)$ is the scale factor which is defined as:

$$I\left(x_m^i\right) = \begin{cases} \dfrac{f_{x_m}\left(x_m^i\right)}{g_{x_m}\left(x_m^i\right)} & f\, R_{xm}{}^i = R_{xm}\left(x_1{}^i, x_2{}^i, \ldots, x_{m-1}{}^i\right) \le x_m{}^i \\ 0 & if\, R_{xm}{}^i = R_{xm}\left(x_1{}^i, x_2{}^i, \ldots, x_{m-1}{}^i\right) > x_m{}^i \end{cases}. \tag{32}$$

The following conclusions are drawn for calculating P_f^{IS} from (28) and (31):

- The number of structural analyses is equal to N and independent from the sample creation of x_m;
- The sample number of x_m is equal to N; and,
- If N values of R_{xm} are known, P_f^{IS} is dependent on the creation of N samples of x_m.

From the above conclusions, EIS is proposed by repeating k - times the creation of N samples of x_m. The unbiased estimate P_f^{EIS} of P_f using EIS is defined as follows:

$$P_f^{EIS} = \frac{1}{k}\sum_{j=1}^{k} P_f^{IS,j}, \tag{33}$$

where $P_f^{IS,j}$ is the unbiased estimate of P_f by using IS corresponding to the sampling creation j^{th} of N samples of x_m; and, k is defined as the duplication factor of EIS.

The flowchart of failure probability analysis of steel frames is given in Fig. 4.

5 Harmony search algorithm

HS is proposed by Geem et al. (2001). Three fundamental elements of HS are the harmony memory matrix (*HM*), the pitch adjustment, and randomization. HS starts by generating the number of variable design vectors (*HMS*) and stores them in *HM* so that they are sorted in terms of objective function value. The member which has the largest objective function value is called the worst member. In iteration steps, a new design vector is created by randomly selecting from the existing matrix of *HM* with probability *HMCR* and by mutating it with a pitch adjustment rate (*PAR),* or by generating a new ones from the variable space with probability (1-*HMCR*). If the objective function value of the new design vector is smaller than that of the worst member of *HM*, it will be chosen to replace the worst member in *HM*. This process is repeated until the maximum number of iterations is reached.

The flowchart of HS algorithm for optimization of steel frames is given in Fig. 5, while the important stages are discussed as follows:

Stage 1: Initialization of problem

In the first stage, the objective function of optimization of steel frames $W(Y)$ is performed as a minimization problem:

$$Min \quad W(Y,X) = \rho\sum_{i=1}^{n}\left(A(y_i)\sum_{q=1}^{n_q} L_q\right), \quad Y = (y_1, y_2, .., y_n), \quad y_i \in [1, UB_i], \tag{34}$$

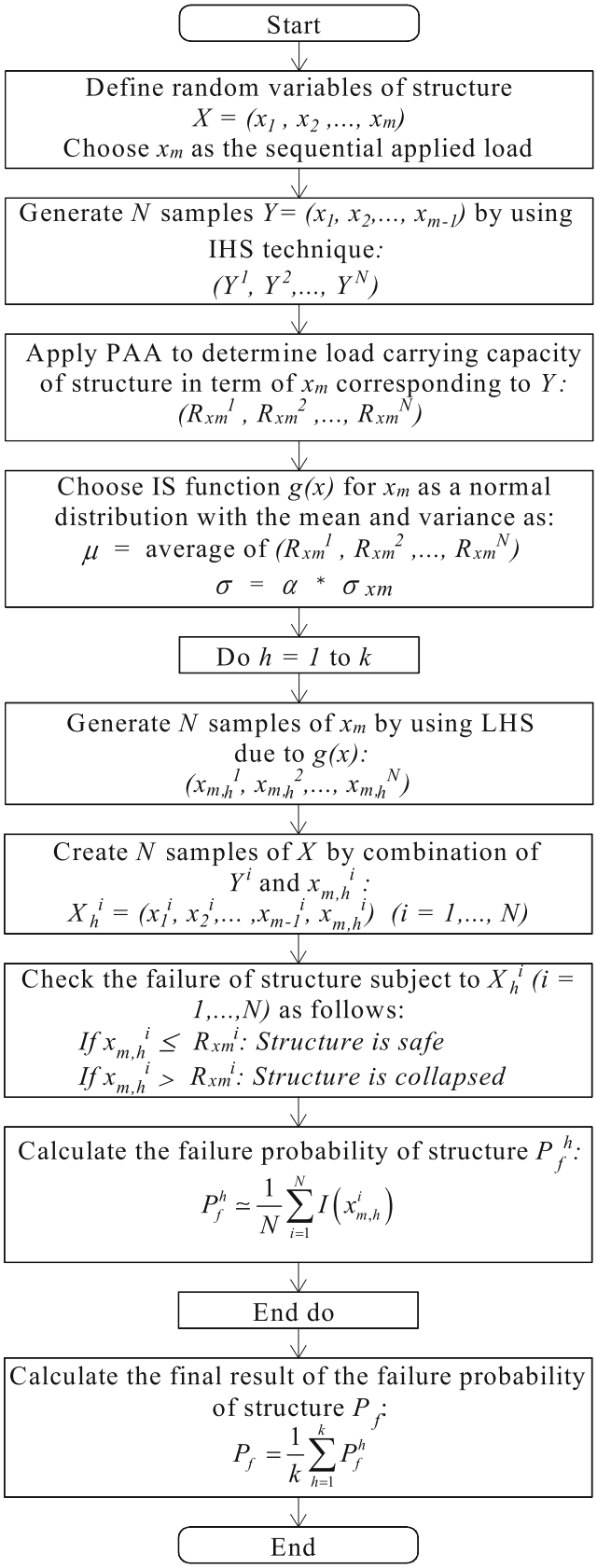

Fig. 4 Flow chart of IHS-EIS procedure

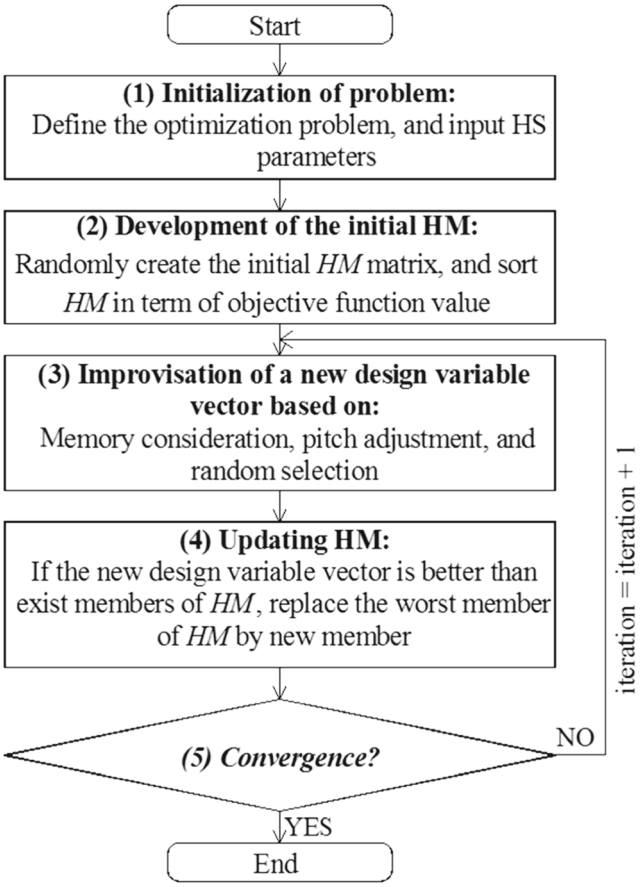

Fig. 5 Flow chart of HS procedure

where UB_i is the number of W-shaped sections of the variable space of y_i. In every iteration of HS, y_i is selected as an integer value in the range $[1, UB_i]$ which represents the position of y_i in the variable space. From the value of y_i, the property parameters of cross-sectional areas of design variables are inputted. To improve the local search capacity of HS, Murren and Khandelwal (2014) proposed the design driven harmony search method (DDHS), in which the space around a design variable is arranged in terms of appropriate section parameter. Since frame members are axial and flexural components, the variable space in this study is sorted in terms of the plastic section modulus Z_x.

The HS parameters are also specified, including harmony memory size *HMS*, harmony consideration rate *HMCR*, the range of pitch adjusting rate [*PAR* min, *PAR* max], and the number of iteration *MaxItr*. The range of bandwidth for mutation is not used in the discrete optimization of steel frames.

Stage 2: Development of the initial HM

Based on the initial parameters of HS, the *HM* matrix is firstly filled by randomly creating *HMS* design variable vectors $Y^j = (y_1^j, y_2^j, .., y_n^j)$ $(j = 1, .., HMS)$, where:

$$y_i^j = rand\text{int}(1, UB_i), \tag{35}$$

in which $rand\,\text{int}(1, UB_i)$ is used for creating the random integer value in the range $[1, UB_i]$.

After generation of the initial design variable vectors, the objective function of problem is evaluated, and *HM* matrix is sorted in terms of objective function from low to high value as follows:

$$HM = \begin{Bmatrix} Y^1 \\ Y^2 \\ \vdots \\ Y^{HMS} \end{Bmatrix} = \begin{bmatrix} y_1^1 & y_2^1 & \cdots & y_n^1 \\ y_1^2 & y_2^2 & \cdots & y_n^2 \\ \vdots & \vdots & \ddots & \vdots \\ y_1^{HMS} & y_2^{HMS} & \cdots & y_n^{HMS} \end{bmatrix}. \tag{36}$$
$$f\left(Y^1\right) \le f\left(Y^2\right) \le \cdots \le f\left(Y^{HMS}\right)$$

The design variable vector which has the largest value of objective function is identified as the worst member of *HM*.

Stage 3: Improvisation of new design variable vector

In this stage, a new design variable vector $Y' = (y_1', y_2', .., y_n')$ is generated based on memory consideration, pitch

Do k = 1, n

rand ~ *U*(0,1)

If (*rand* < *HMCR*)

y_k' is randomly chosen from $\left\{y_k^1, y_k^2, ..., y_k^{HMS}\right\}$

Else

y_k' is newly generated in the range $\left[1, UB_k\right]$

End if

End do

adjustment, and random selection. The process of generating a new design variable vector is called improvisation. $Y^{'}$ is assigned due to the rule of memory consideration and the value of *HMCR* as follows:

If $y_k^{'}$ is chosen from $\{y_k^1, y_k^2, \ldots, y_k^{HMS}\}$, the rule of pitch adjustment will be applied with a probability *PAR*, where *PAR* is linearly adjusted with generation number as follows:

$$PAR(current\,iteration) = PAR\min + \frac{current\,iteration}{total\,iteration} \times (PAR\max - PAR\min). \quad (37)$$

The modification of $y_k^{'}$ is set as:

$$y_k^{'} = \begin{cases} y_k^{'} + rand\,\mathrm{int}(1,3) & if\ (rand < 0.5) \\ y_k^{'} - rand\,\mathrm{int}(1,3) & if\ (rand \geq 0.5) \end{cases}. \quad (38)$$

Equation (38) indicates that $y_k^{'}$ is mutated with an integer step of random search direction. The step size in this study is chosen in the range [1, 3] due to the suggestion of Degertekin (2008).

To improve the harmony search method, *HMCR* and *PAR* of components of $Y^{'}$ are determined by applying the adaptive harmony search method (AHS) proposed by Hasançebi et al. (2010a, b) as follows:

$$\begin{cases} HMCR\left(y_j^{'}\right) = \left(1 + \dfrac{1-\overline{HMCR}}{\overline{HMCR}} \exp(-\gamma N(0,1))\right)^{-1} \\ PAR\left(y_j^{'}\right) = \left(1 + \dfrac{1-\overline{PAR}}{\overline{PAR}} \exp(-\gamma N(0,1))\right)^{-1} \end{cases} (j = 1, .., n), \quad (39)$$

where $\overline{HMCR}$ and $\overline{PAR}$ are the average values of the memory consideration rate and pitch adjustment rate, respectively, which are used for controlling mutation of $Y^{'}$; and, $\gamma \in [0.25, 0.50]$ is a scalar.

To reduce the computational time of structural analysis, the matrix *HMstor* is created to store all design vectors in every iteration. If $Y^{'}$ is the same with one member of *HMstor*, it will be discarded and a new design variable vector is generated again; otherwise, $Y^{'}$ is stored in *HMstor*.

Stage 4: Updating HM

If the objective function value of the worst member of *HM* is larger than ones of $Y^{'}$, it will be replaced by $Y^{'}$. Then, *HM* is sorted again in terms of objective function from low number to high number.

Stage 5: Termination of optimization process

Stages 3 and 4 are repeated until the maximum number of objective function evaluations is reached or the best design shows no further improvements during a specific number of iterations. The member of *HM* which has the smallest value of objective function is chosen as the final result of HS optimization process.

6 Proposed RBDO procedure

In this section, an effective RBDO procedure for space steel frames is proposed by a hybrid approach from HS and IHS-EIMS as illustrated in Fig. 6.

As can be seen in Fig. 6, the proposed procedure is divided into five big steps: (1) initializing the optimization problem, (2) generating the deterministic *HM*, (3) generating the probabilistic *HM*, (4) improvisation of new design variable vector, and (5) updating *HM*. The deterministic *HM* means that all members of *HM* satisfy deterministic constraints of optimization. The

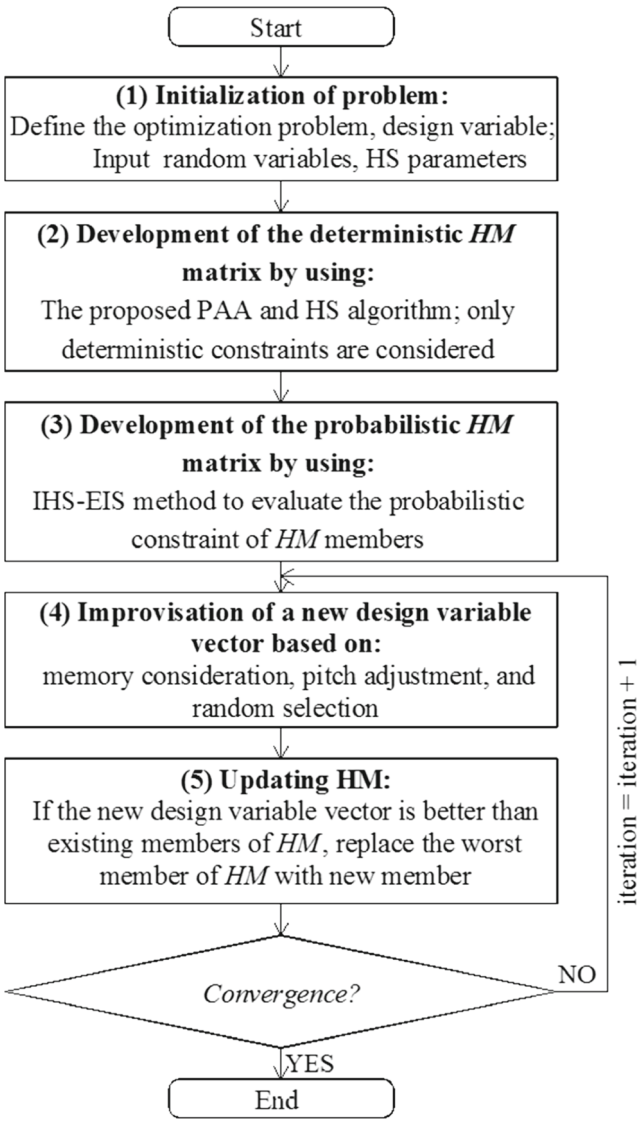

Fig. 6 Flow chart of the proposed procedure for optimization of space steel frames

probabilistic *HS* means that all members of *HM* satisfy deterministic and probabilistic constraints of optimization.

In the first step, the objective function, constraints, and design variables of the optimization are defined. The information of random variables and HS parameters is inputted.

In the second step, the deterministic *HM* is developed by using HS algorithm considering only deterministic constraints as follows:

1. Generate the initial *HM*
2. Evaluate the deterministic constraints of members of *HM* by using PAA
3. Calculate the deterministic objective function of members
4. Sort *HM* by deterministic objective function from low to high value
5. Generate a new design variable vector based on HS operators by using memory consideration, pitch adjusting, and randomization
6. Repeat steps 2 and 3 to evaluate objective function of the new member
7. Replace the worst member of *HM* by new member if improved
8. Sort *HM* in terms of deterministic objective function from low to high value
9. Repeat 5–8 until the worst member of *HM* satisfies all deterministic constraints

In the third step, the probabilistic *HM* is developed as follows:

1. Evaluate the probabilistic constraint of members of the deterministic *HM* by using IHS-EIS
2. Calculate the objective function of members of the deterministic *HM*
3. Sort the deterministic *HM* by objective function from low to high value
4. Generate a new design variable vector based on HS operators by using memory consideration, pitch adjusting, and randomization
5. Evaluate deterministic constraints of the new member
6. Evaluate the probabilistic constraint of the new member if it satisfies all deterministic constraints; otherwise, go back step 4
7. Evaluate objective function of the new member
8. Replace the worst member of *HM* with new member if improved
9. Sort *HM* in terms of objective function from low to high value
10. Repeat 4–9 until the worst member of *HM* satisfies all constraints

Since probabilistic *HM* is developed, the new design variable vector is firstly created by using HS operators in the fourth step. The deterministic objective function of the new member is then evaluated by using PAA. The probabilistic constraint of new member is only evaluated if its deterministic objective function is smaller than the objective function of the worst member of *HM*. *HM* is updated if the objective function of the new member is smaller than that of the worst member of *HM* in the fifth step.

The optimization is terminated when the total number of iterations is reached or the best design shows no further improvements during a specific number of iterations.

7 Numerical examples

7.1 Verification of IHS-EIS

The PAA method presented in Section 3 has been implemented in the practical advanced analysis program (PAAP) (Thai and Kim 2009) to calculate the load-carrying capacity of steel frames, so only IHS-EIS is verified in this study through three mathematical examples and one planar steel frame. The mathematical examples are modified from the published problems in order to reach the target failure probability of 0.1%, which value is often used for reliability-based design of structure. MCS, IS, and Subset simulation (SS) methods are employed for comparison. SS is performed by using the Matlab code which is provided by Li and Cao (2016), and the partial failure probability P_i is equal to 0.1. The duplication factor k of IHS-EIS for these examples is equal to 2000.

7.1.1 Mathematical examples

Three limit state functions (LSFs) are considered in this section. The original problems were proposed by Engelund and Rackwitz (1993) and used by many authors in the literature due to their complexities for solving by using FORM/SORM.

Table 1 Results of three mathematical examples with the same number of samples

LSF No.	Samples	MCS with 2 million samples (Accurate P_f(%))	SS		IS		Proposed method EIS, $k=2000$		Proposed method IHS-EIS, $k=2000$	
			P_f (%)	COV of P_f	P_f (%)	COV of P_f	P_f (%)	COV of P_f	P_f (%)	COV of P_f
1	840	0.139	0.191	0.58	0.133	1.11	0.141	0.30	0.136	0.03
2	1110	0.111	0.150	0.65	0.109	1.39	0.116	0.33	0.117	0.26
3	1400	0.150	0.200	0.44	–	–	0.150	0.52	0.154	0.39

Table 2 Results of three mathematical examples with the same COV of P_f

LSF No.	MCS		SS		IS		Proposed method EIS, $k=2000$		Proposed method IHS-EIS, $k=2000$	
	Sample	COV of P_f	Sample	COV of P_f	Sample	COV of P_f	Sample	COV of P_f	Sample	COV of P_f
1	1,000,000	0.03	42,000	0.10	100,000	0.14	10,000	0.077	500	0.032
2	15,000	0.25	5040	0.27	34,000	0.26	1800	0.27	1110	0.26
3	10,000	0.32	1960	0.39	–	–	3000	0.44	1400	0.39

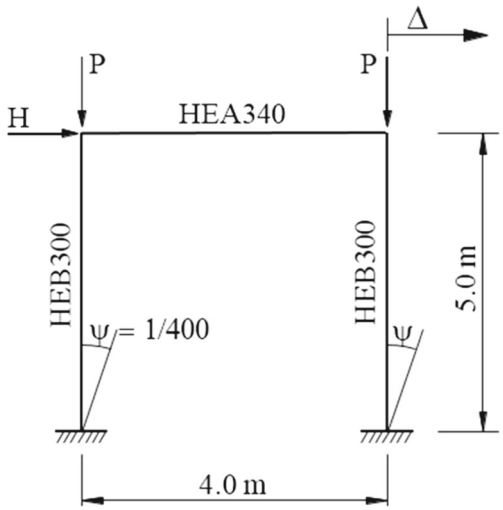

Fig. 7 Vogel portal frame

a. Multiple failure points with two random variables

$$LSF_1 = X_1X_2 - PL, \tag{40}$$

in which : $P = 14.614$, $L = 10.0$,
$X_1 \sim N(31064.4, 4659.6)$,
and $X_2 \sim N\left(0.0104, 1.56 \times 10^{-3}\right)$.

In this example, X_2 is selected to perform IS and IHS-EIS techniques.

b. Noisy limit state function with six random variables

$$LSF_2 = X_1 + 2X_2 + 2X_3 + 2X_4 - 5X_5 - 5X_6 + 0.01\sum_{i=1}^{6}\sin(100X_i), \tag{41}$$

in which $X_1 \sim N(50, 5)$,
$X_2, X_3, X_4 \sim N(120, 12)$,
$X_5 \sim N(50, 15)$,
and $X_6 \sim N(40, 12)$.

X_6 is selected in this example to perform IS and IHS-EIS.

c. Noisy limit state function with 17 random variables

This example is the modification of the example 2 for high dimensions of random variables. The LSF is written as follows:

$$LSF_3 = \sum_{i=1}^{7} X_i - \sum_{i=8}^{17} X_i + 0.001\sum_{i=1}^{17}\sin(100X_i), \tag{42}$$

in which $X_1 \sim N(80, 8)$,
$X_i \sim N(120, 12)\ (i = 2, 7)$,
$X_i \sim N(80, 24)\ (i = 8, 12)$,
and $X_i \sim N(40, 12)\ (i = 13, 17)$.

In this example, X_{17} is chosen for performing IS and IHS-EIS.

Tables 1 and 2 show the numerical results with 500 independent runs for each value. MCS with 2 million samples is used to calculate the accurate P_f. As can be seen in Table 1, the

Table 3 Statistical properties of random variables for Vogel portal frame

Properties	Variables	Nominal	Mean/nominal	COV	Distribution	Reference
Material	E	205 (GPa)	1.00	0.04	Lognormal	Bartlett et al. (2003)
	F_y	235 (MPa)	1.10	0.06	Lognormal	Bartlett et al. (2003)
Cross-section	A_b	0.0133 (m2)	1.00	0.05	Normal	Ellingwood et al. (1982)
	I_b	2.769E-4 (m4)	1.00	0.05	Normal	Ellingwood et al. (1982)
	A_c	0.0149 (m2)	1.00	0.05	Normal	Ellingwood et al. (1982)
	I_c	2.517E-4 (m4)	1.00	0.05	Normal	Ellingwood et al. (1982)
Loading	P	2240 (KN)	1.05	0.10	Normal	Ellingwood et al. (1982)
	H	28 (KN)	0.92	0.37	Gumbel	Ellingwood et al. (1982)

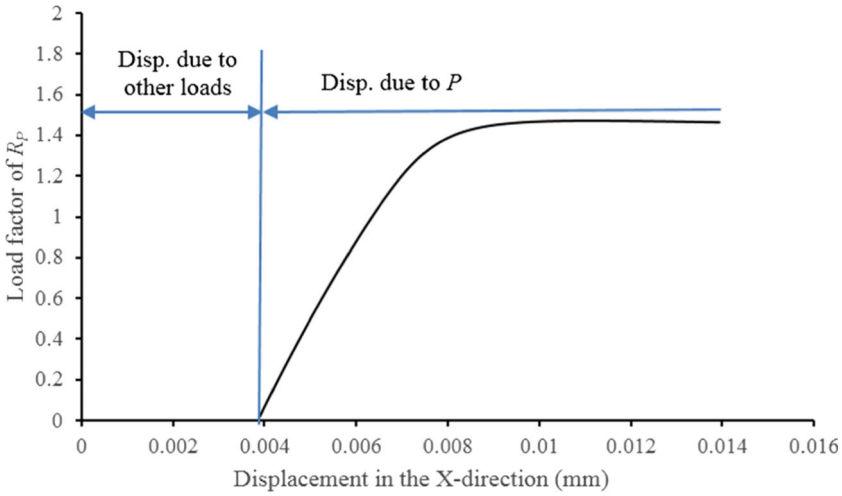

Fig. 8 Load-roof displacement response of Vogel portal frame

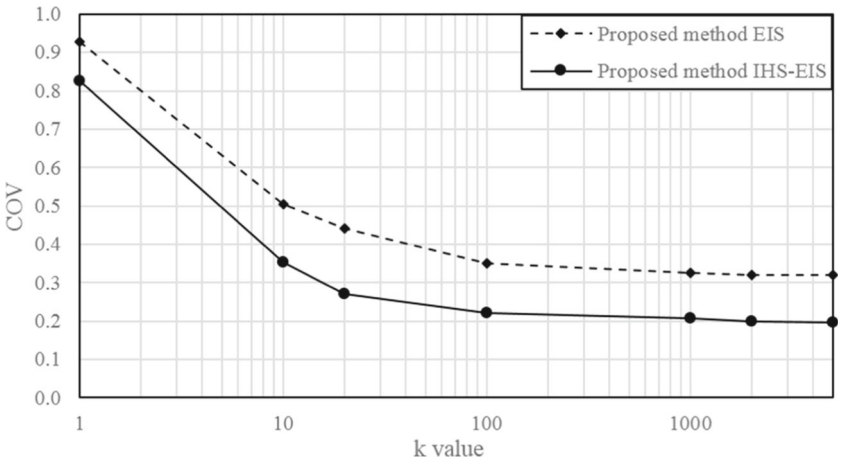

Fig. 9 Relationship between k value with COV of structural failure probability of Vogel portal frame

means of P_f by using IS and the proposed methods (EIS, IHS-EIS) are almost equal to the accurate values, while those by using SS are 34–37% higher than the accurate ones. Furthermore, the values of coefficient of variation (COV) of P_f of IHS-EIS are smaller than those of SS and IS, especially in examples 1 and 2 where the number of random variables are 2 and 6, respectively. In particular, in example 2, COV of 0.26 of P_f by using IHS-EIS is equal to 40 and 18.7% of those by using SS and IS, respectively. As can be observed from Table 2, the sample numbers of IHS-EIS in the examples 2 and 3 are 80.15 and 28.57% lower than those of SS, respectively. The sample number of 500 of IHS-EIS in the example 1

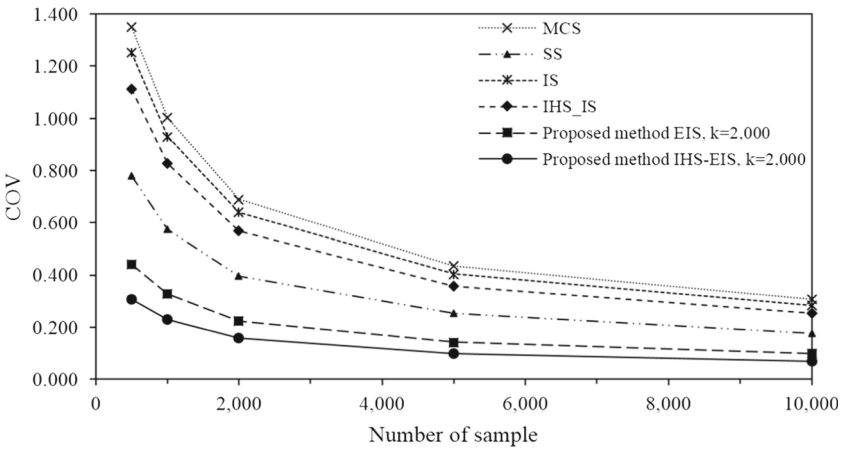

Fig. 10 COV of structural failure probability of reliability analysis methods for Vogel portal frame

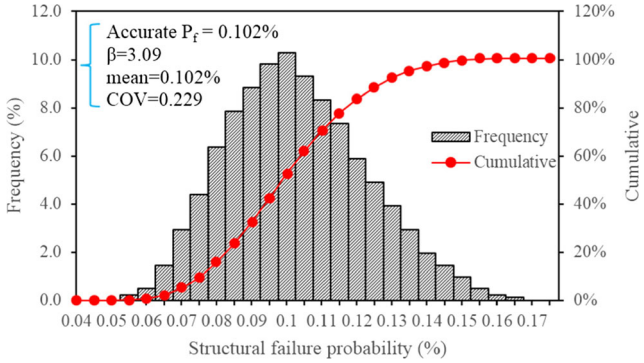

Fig. 11 Histogram of failure probability of Vogel portal frame using the proposed method IHS-EIS ($k = 2000$) with 1000 samples

1.470, as can be obtained from Fig. 8. Therefore, the IS distribution of P is chosen as a normal distribution with $mean = 1.470 * mean\ of\ P$ and $COV = 5 * COV\ of\ P$. Figure 9 shows the relationship between k and COV of P_f by using EIS and IHS-EIS with 1000 samples. It can be seen that the COV value is converged when k is larger than 2000. Thus, the value of k is chosen as 2000.

The relationship of COV of P_f and sample number is shown in Fig. 10 with 500 independent evaluations for each value. As can be seen in this figure, COV of P_f by using IHS-EIS is 77 and 60% lower than those by using MCS and SS, respectively, while IS is not much effective.

Table 4 HS parameters and design information of deterministic optimization examples

Example	Design space	HS parameters	Constraints
Two-bay three-story (2 × 3) planar frame	Beam bracing: *L/6* Beam: all W-shapes Column: W10	*HMS* = 25 *HMCR* = 0.8 *PAR* = 0.4 *MaxItr* = 2000	Strength: Yes Drift: No Geometry: No
Five-bay fourteen-story (5 × 14) planar frame	Beam bracing: *L/6* Beam: all W-shapes Column: W12, W14, W18, W21, W24, W27	*HMS* = 100 *HMCR* = 0.8 *PAR* = 0.4 *MaxItr* = 25,000	Strength: Yes Drift: *H/400* Geometry: Yes

is greatly smaller than 42,000 of SS since only 2 random variables are considered.

7.1.2 Vogel portal frame

The geometric dimensions and section properties of the frame are presented in Fig. 7, while the information of eight random variables is given in Table 3. The accurate value of P_f is equal to 0.1017%. The vertical load P is used to perform IS, EIS, and IHS-EIS. The ultimate load factor of the frame in terms of P due to the mean values of the random variables is equal to

The frequency histogram of P_f by using IHS-EIS with 1000 samples is shown in Fig. 11. The mean value of 0.102% of P_f distribution is almost equal to the accurate value. In addition, the mean value of 0.142% of P_f by using SS is about 40% higher than the accurate P_f. Hence, IHS-EIS can capture the failure probability more precisely than SS.

It should be noted that SS is based on Markov Chain Monte Carlo (MCMC) technique which generates samples one by one, so parallel computing cannot be performed to reduce the computational cost of SS. In the computational cost view of point, the proposed method hence is more effective than SS in structural optimization. Therefore, it can be concluded that

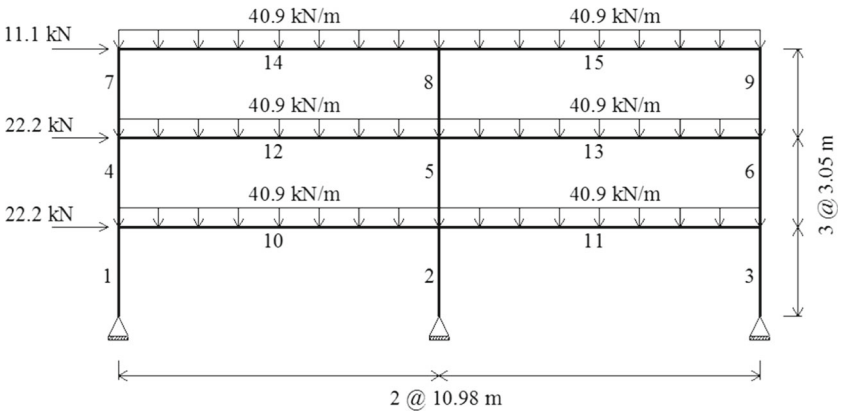

Fig. 12 Two-bay three-story planar frame

Table 5 Optimal results of two-bay three-story planar frame

Element group	GA (Pezeshk et al. 2000)	ACO (Camp et al. 2005)	HS (Degertekin 2008)	DDHS (Murren and Khandelwal 2014)	HS in this study	
					Linear analysis	Advanced analysis
Beam	W24 × 62	W24 × 62	W21 × 62	W24 × 62	W24 × 62	W21 × 44
Column	W10 × 60	W10 × 60	W10 × 54	W10 × 60	W10 × 60	W10 × 45
Wt. (lb)	18,792	18,792	18,292[a]	18,792	18,792	13,660
Wt. (kN)	83.6	83.6	81.4[a]	83.6	83.6	60.77
Avg. number of analyses	780	2200	853	200	231	243
Normalized strength capacity	–	–	–	–	1.001	1.002
Number of times optimum results obtained	5/30	84% of total simulations	<100% of total simulations [b]	100/100	100/100	100/100

[a] The design is infeasible

[b] The average weight of 30 different designs is 18,784 lb, with a standard deviation of 411 lb

the proposed method for structural reliability analysis is effective and accurate.

7.2 Deterministic optimization of steel frames

Two planar frames are investigated in this section to illustrate the accuracy and efficiency of the proposed procedure for deterministic optimization of steel frames. In addition, the comparison of linear and nonlinear inelastic analyses is shown. The HS parameters and design variable spaces are given in Table 4. All frames use ASTM A992 steel with $F_y = 248\,MPa$ and $E = 200\,GPa$.

7.2.1 Two-bay three-story planar frame

The frame has 15 members which are split into 2 member groups, beams and columns, as shown in Fig. 12. This frame was optimized by Pezeshk et al. (2000), Camp et al. (2005),

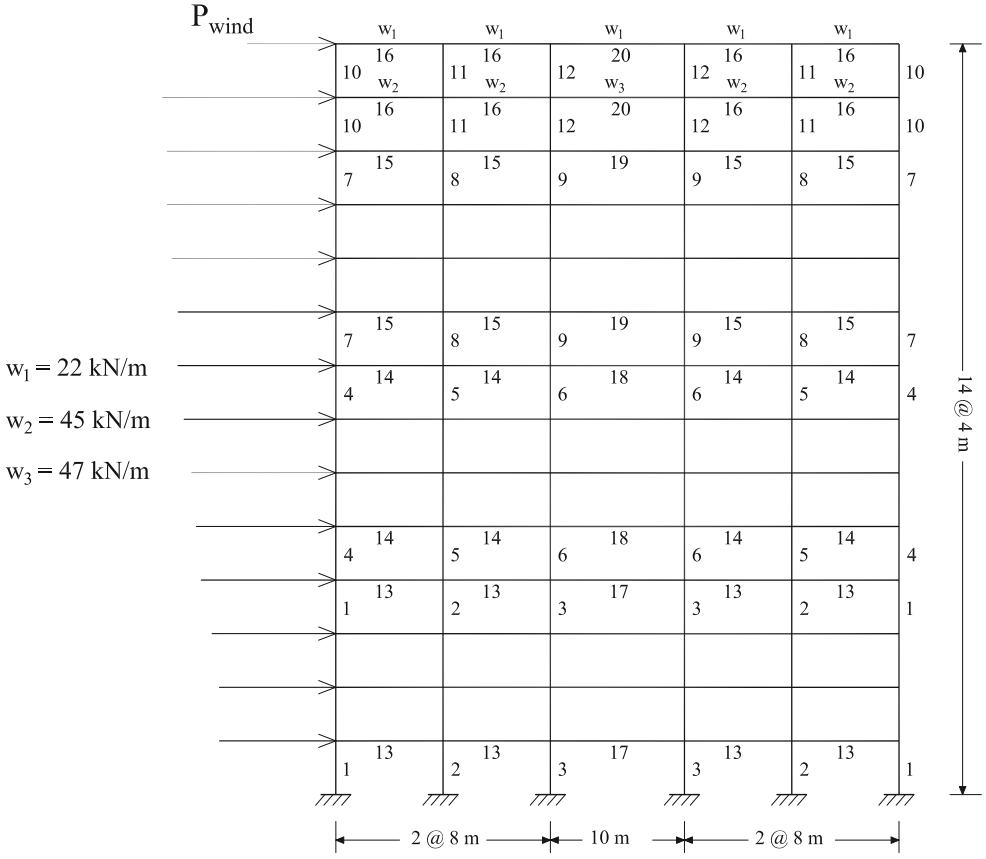

Fig. 13 Five-bay fourteen-story planar frame

Table 6 Equivalent static wind loads of five-bay fourteen-story planar frame

Story	Equivalent static wind load (kN)
1	17.37
2	17.37
3	18.46
4	20.09
5	20.82
6	21.54
7	22.63
8	23.54
9	23.54
10	24.45
11	25.17
12	25.17
13	25.90
14	13.22

of this frame using linear analysis is W24 × 62 for beams and W10 × 60 for columns, which was demonstrated by Pezeshk et al. (2000) by checking all possibilities of design variables.

Table 5 shows the optimization results obtained from 100 evaluations for each value. It can be seen from this table that the proposed procedure successfully captures the optimum design in the average of 231 and 243 iterations corresponding to using linear and nonlinear inelastic analyses, respectively. These are much better than the 780 iterations of GA (Pezeshk et al. 2000), 2200 iterations of ACO (Camp et al. 2005), and 853 iterations of HS in (Degertekin 2008), and similar to 200 iterations of DDHS (Murren and Khandelwal 2014). In addition, the optimum design of the frame using nonlinear inelastic analysis is W21 × 44 for beams, W10 × 45 for columns, and

Table 7 Optimal results of five-bay fourteen-story planar frame

	Alberdi and Khandelwal (2015)						HS in this study	
	ACO	GA	DDHS	PSO	ISA	TS	Linear analysis	Nonlinear inelastic analysis
Avg. Wt. (kN)	1030.1	1040.4	779.33	1244.40	1447.0	797.20	791.67	790.83
Std. Wt. (kN)	32.30	95.70	6.39	262.9	278.4	13.40	11.16	10.73
Percent feasible	100.0	100.0	100.0	97.6	64.6	100.0	100.0	100.0

Degertekin (2008), and Murren and Khandelwal (2014) by using GA, ACO, HS, and DDHS, respectively. Only strength constraint is considered in this example. The optimum design total weight of 60.77 *kN*. This optimum weight is equal to 72.7% of one using linear analysis. The reason is that the nonlinear inelastic analysis considers the inelastic force

Table 8 Best optimal designs of five-bay fourteen-story planar frame

Member group	Alberdi and Khandelwal (2015)						HS in this study	
	ACO	GA	DDHS	PSO	ISA	TS	Linear analysis	Nonlinear inelastic analysis
1	21 × 101	24 × 104	14 × 82	27 × 129	21 × 147	18 × 76	14 × 82	14 × 82
2	24 × 131	21 × 122	21 × 132	18 × 143	27 × 161	24 × 131	21 × 132	21 × 132
3	21 × 147	24 × 146	14 × 145	21 × 166	24 × 192	24 × 146	14 × 145	14 × 145
4	18 × 86	24 × 84	12 × 65	24 × 84	24 × 94	18 × 76	12 × 65	12 × 65
5	21 × 101	18 × 97	14 × 90	27 × 129	14 × 109	27 × 102	14 × 90	14 × 90
6	14 × 120	14 × 120	14 × 109	18 × 158	18 × 119	24 × 104	14 × 109	14 × 109
7	12 × 87	14 × 53	12 × 50	21 × 68	21 × 73	14 × 53	12 × 50	12 × 50
8	14 × 109	18 × 119	14 × 61	21 × 83	21 × 83	24 × 68	14 × 61	14 × 61
9	12 × 96	12 × 82	12 × 65	21 × 147	21 × 101	18 × 76	12 × 65	12 × 65
10	24 × 117	14 × 30	14 × 30	21 × 132	24 × 131	12 × 30	14 × 30	14 × 30
11	12 × 65	24 × 55	12 × 30	27 × 114	12 × 65	12 × 30	12 × 30	12 × 30
12	18 × 130	12 × 40	14 × 38	27 × 178	24 × 146	14 × 43	14 × 38	14 × 38
13	21 × 44	21 × 44	21 × 44	21 × 44	16 × 40	21 × 44	21 × 44	21 × 44
14	18 × 40	24 × 55	21 × 44	14 × 48	21 × 73	18 × 35	21 × 44	21 × 44
15	18 × 35	16 × 36	18 × 35	16 × 36	16 × 50	18 × 35	18 × 35	18 × 35
16	16 × 36	18 × 35	18 × 35	14 × 48	12 × 40	18 × 35	18 × 35	18 × 35
17	12 × 72	18 × 50	21 × 48	21 × 57	21 × 57	21 × 48	21 × 48	21 × 48
18	16 × 89	12 × 79	21 × 50	16 × 100	21 × 57	21 × 48	21 × 50	21 × 50
19	16 × 50	18 × 65	21 × 44	16 × 57	18 × 60	21 × 44	21 × 44	21 × 44
20	16 × 45	18 × 46	21 × 44	21 × 55	21 × 44	18 × 50	21 × 44	21 × 44
Weight (kN)	925.14	838.05	756.55	1043.4	1042.7	756.84	756.55	756.55
Normalized strength capacity	–	–	–	–	–	–	1.001	1.734
Max. normalized story drift							0.996	0.996
Max. normalized geometry							0.960	0.960

Table 9 Design summary of RBDO of steel frames

	Two-story space frame	Six-story space frame
Design space	Beam: all W-shapes Column: W10, W12	Beam: all W-shapes Column: W14, W18, W21, W24
IHS-EIS parameters	$k = 2000$ Number of samples = 1000	$k = 2000$ Number of samples = 1000
Constraints	Strength: Yes Drift: *H/400* Geometry: Yes	Strength: Yes Drift: *H/400* Geometry: Yes
Termination criteria	Total function evaluation = 2000 Number of function evaluation for no improvement of best member = 500	Total function evaluation = 2000 Number of function evaluation for no improvement of best member = 1000
HS parameters	*HMS* = 25 *HMCR* = 0.8 *PAR* = 0.4 *MaxItr* = 2000	*HMS* = 50 *HMCR* = 0.8 *PAR* = 0.4 *MaxItr* = 5000
GA	Population = 50 Iteration = 40 Mutation = 0.8 Crossover: Uniform technique with crossover rate = 0.5	Population = 100 Iteration = 100 Mutation = 0.8 Crossover: Uniform technique with crossover rate = 0.5
Micro-GA	Population = 10 Iteration = 200 Mutation: No Crossover: Uniform technique with crossover rate = 0.5 Elitism scheme: Yes	Population = 10 Iteration = 500 Mutation: No Crossover: Uniform technique with crossover rate = 0.5 Elitism scheme: Yes
PSO	Number of particle = 20 Iteration = 100 $c_1 = 2$ $c_2 = 4$ Velocity limit scheme: Yes Evaluate center of gravity: Yes Initialize by Quasi-Monte Carlo: Yes Local random search: Yes	Number of particle = 50 Iteration = 100 $c_1 = 2$ $c_2 = 4$ Velocity limit scheme: Yes Evaluate center of gravity: Yes Initialize by Quasi-Monte Carlo: Yes Local random search: Yes

distribution while the linear analysis cannot. In addition, the satisfaction of the strength constraint of the best frame designs is shown in Table 5 by using the normalized strength capacity, which is defined as the ratio of load-carrying capacity of the structure and applied loads. In this table, this value greater than 1 means that the strength constraint is satisfied.

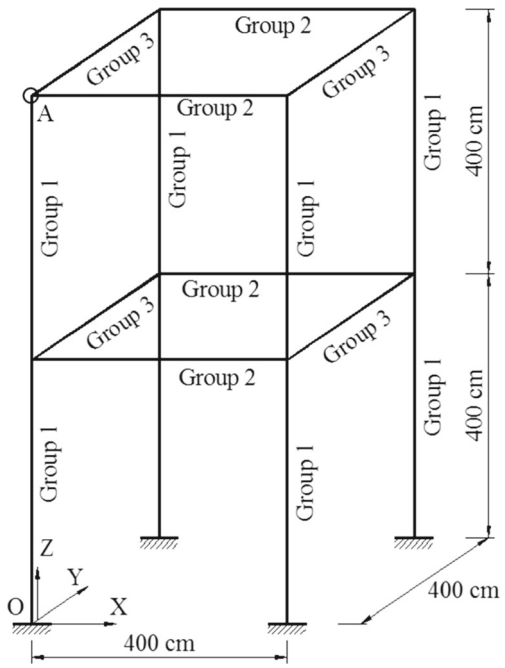

Fig. 14 Two-story space frame

7.2.2 Five-bay fourteen-story planar frame

The frame has 174 members which are split into 20 member groups as shown in Fig. 13. This frame was optimized by Alberdi and Khandelwal (2015) using many different metaheuristic algorithms. All strength, drift, and geometric construction constraints are considered in this example. The equivalent static wind loads for this frame are given in Table 6.

The optimization results obtained from 100 evaluations for each value are presented in Table 7, while the best designs are given in Table 8. It can be seen in Table 7 that the average and standard deviation of the optimum frame weight of the proposed procedure using linear analysis are 791.67 and 11.16 *kN*, respectively. These results are better than those of ACO, GA, PSO, and ISA, and similar to those of DDHS and TS, which are given in Alberdi and Khandelwal (2015). In addition, the average of 790.83 *kN* of the optimum frame weight using nonlinear inelastic analysis is similar to the one using linear analysis. The reason is that the optimum design of the

Table 10 Statistical properties of random variables for two-story space frame

Properties	Variables	Nominal	Mean/nominal	COV	Distribution	Reference
Material	E	200 (GPa)	1.00	0.04	Lognormal	Bartlett et al. (2003)
	F_y	248 (MPa)	1.10	0.06	Lognormal	Bartlett et al. (2003)
Cross-section	A_i	–	1.00	0.05	Normal	Ellingwood et al. (1982)
	I_i	–	1.00	0.05	Normal	Ellingwood et al. (1982)
Loading	DL	50 (KN/m)	1.05	0.10	Normal	Ellingwood et al. (1982)
	LL	30.5 (KN/m)	1.00	0.10	Normal	Ellingwood et al. (1982)
	W	30 (KN)	0.92	0.37	Gumbel	Ellingwood et al. (1982)

Table 11 RBDO results of two-story space frame

	GA	Micro-GA	PSO	Proposed method 1	Proposed method 2
Avg. Wt. (kN)	50.81	47.34	55.63	41.23	41.52
Std. Wt. (kN)	4.59	4.23	6.83	2.22	2.53
Avg. computational time (h)	12.89	11.93	13.85	13.67	0.69
Best design	12 × 53, 18 × 35, 14 × 22	12 × 53, 18 × 35, 14 × 22	12 × 53, 18 × 35, 14 × 22	12 × 53, 18 × 35, 14 × 22	12 × 53, 18 × 35, 14 × 22
Weight of best design (kN)	38.19	38.19	38.19	38.19	38.19
Normalized strength capacity of best design	1.535	1.535	1.535	1.535	1.535
Max. normalized store drift of best design	0.553	0.553	0.553	0.553	0.553
Max. normalized geometry of best design	0.601	0.601	0.601	0.601	0.601
Normalized failure probability of best design	0.983	0.932	0.869	0.873	0.972

frame is controlled by the inter-story drift constraints which are calculated by using elastic analysis in both of the optimization using linear and nonlinear inelastic analyses. Furthermore, the satisfaction of the strength, story drift, and geometric constraints of the best frame designs are presented in Table 8. The maximum normalized story drift is defined as the ratio of the maximum value of structural story drifts and the allowable story drift, and the maximum normalized geometry is the maximum value of geometric constructional constraints. As can be seen in this table, the normalized strength capacity is greater than 1, while the maximum normalized story drift and maximum normalized geometry are smaller than 1. This means that all constraints are satisfied.

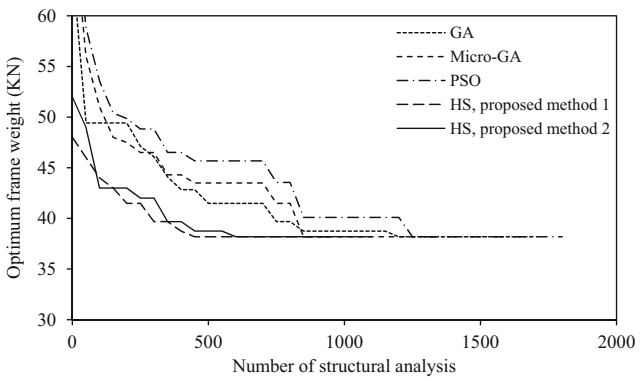

Fig. 15 Convergence histories of the best designs of two-story space frame

From the two aforementioned examples of steel frames, it can be concluded that the proposed optimization procedure is effective and robust. Furthermore, the optimum designs using nonlinear inelastic analysis are better than those using linear elastic analysis. Therefore, using nonlinear inelastic analysis in optimization of steel frames is preferable.

7.3 Reliability-based design optimization of steel frames

Two space steel frames are investigated in this section to illustrate the accuracy and efficiency of the proposed procedure for RBDO of frames. Only nonlinear inelastic analysis is considered. GA, micro-GA, and PSO are employed for comparison, which are performed using the latest FORTRAN code versions developed by Carroll (2001) for GA and micro-GA and Tada (2007) for PSO.

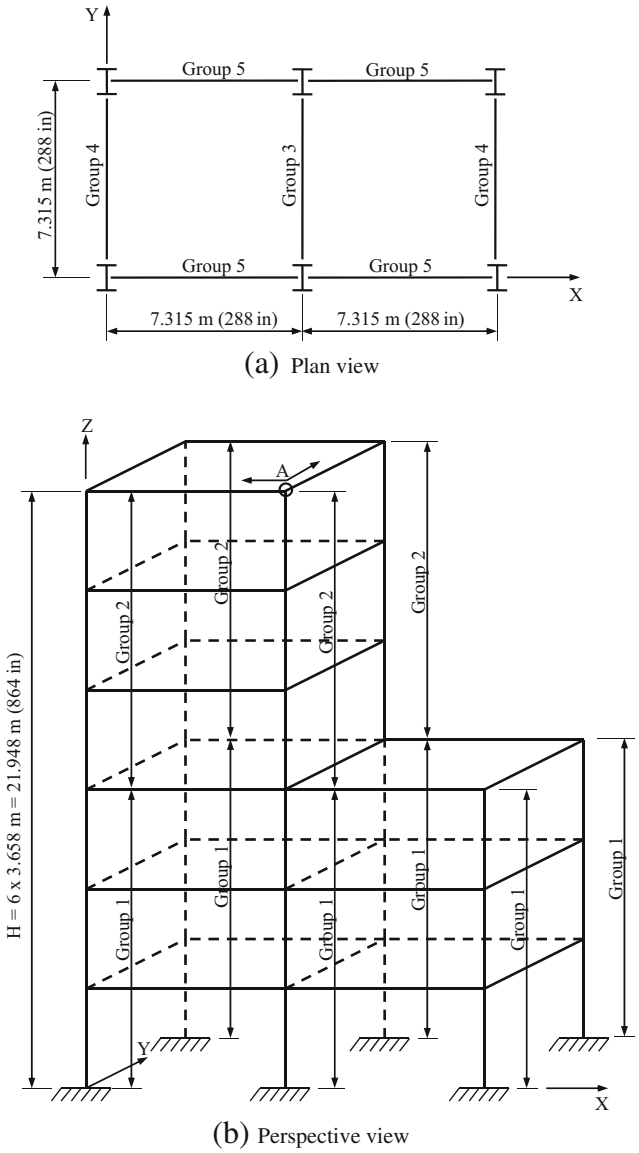

Fig. 16 Six-story space frame. **a** Plan view. **b** Perspective view

The proposed procedure is considered in two options: proposed method 1 is that probabilistic constraint is evaluated in all design samples, and proposed method 2 is to use the fully proposed procedure. The design summary and metaheuristic parameters are given in Table 9. Both frames are optimized according to the load combinations for the serviceability of $(DL_n + 0.5LL_n + 0.7W_n)$ and for the strength and failure probability of $(1.2DL_n + 0.5LL_n + 1.6W_n)$, in which DL_n, LL_n, and W_n are the nominal values of dead, live, and wind loads, respectively. Parallel computing is also used for probability constraint evaluation by using the shared memory programming model OpenMP. For these examples, 10 processors of the computer configuration (Intel® Core™ i7-3930 K CPU@3.20Hz 4.20Hz) are used. Each method is run 50 times in order to investigate the efficiency and accuracy of the methods.

7.3.1 Two-story space frame

This frame with three design variables is shown in Fig. 14. Wind loads are converted into point loads at every beam-column joint in the *X*-direction. The total number of random variable is therefore equal to 11. The information of random variables is given in Table 10.

The RBDO results of the frame are shown in Table 11. As can be seen in this table, proposed method 1 produces the lowest average and standard deviation of the optimum frame weight, 41.23 *kN* and 2.22 *kN*, respectively. These are similar to the average of 41.52 *kN* and the standard deviation of 2.53 *kN* of the optimum frame weight by using proposed method 2. However, the average computational time of 0.69 h of proposed method 2 is much less than those of 12.89, 11.93, 13.85, and 13.67 h of GA, micro-GA, PSO, and proposed method 1, respectively. The satisfaction of probabilistic and deterministic constraints of the best frame designs is also shown in the Table 11, in which the normalized failure probability is the ratio of structural failure probability and the allowable failure probability value. In this table, the normalized strength capacity is greater than 1, while the maximum normalized story drift, maximum normalized geometry, and normalized failure probability are smaller than 1. This means that all constraints are satisfied. In addition, Fig. 15 shows the convergence histories of the best optimum designs of the frame.

Table 12 Statistical properties of random variables for six-story space frame

Properties	Variables	Nominal	Mean/ nominal	COV	Distribution	Reference
Material	E	200 (GPa)	1.00	0.04	Lognormal	Bartlett et al. (2003)
	F_y	248 (MPa)	1.10	0.06	Lognormal	Bartlett et al. (2003)
Cross-section	A_i	–	1.00	0.05	Normal	Ellingwood et al. (1982)
	I_i	–	1.00	0.05	Normal	Ellingwood et al. (1982)
Loading	DL	19.5 (kN/m)	1.05	0.10	Normal	Ellingwood et al. (1982)
	LL	10.5 (kN/m)	1.00	0.10	Normal	Ellingwood et al. (1982)
	W	20 (kN)	0.92	0.37	Gumbel	Ellingwood et al. (1982)

Table 13 RBDO results of six-story space frame

	GA	Micro-GA	PSO	Proposed method 1	Proposed method 2
Avg. Wt. (kN)	267.56	261.37	280.37	245.11	246.42
Std. Wt. (kN)	19.23	17.79	23.67	5.62	6.21
Avg. computational time (h)	32.58	31.73	35.47	34.66	1.84
Best design	24 × 84, 21 × 55, 21 × 57, 24 × 55, 12 × 19	24 × 84, 21 × 55, 21 × 57, 24 × 55, 12 × 19	24 × 94, 21 × 55, 21 × 48, 24 × 55, 12 × 19	24 × 84, 21 × 48, 21 × 57, 24 × 55, 12 × 19	24 × 84, 21 × 48, 21 × 57, 24 × 55, 12 × 19
Weight of best design (kN)	242.65	242.65	246.79	238.07	238.07
Normalized strength capacity of best design	1.263	1.263	1.396	1.262	1.262
Max. normalized store drift of best design	0.675	0.675	0.743	0.678	0.678
Max. normalized geometry of best design	0.853	0.853	0.991	0.861	0.861
Normalized failure probability of best design	0.956	0.889	0.935	0.896	0.963

7.3.2 Six-story space frame

This frame with five design variables is shown in Fig. 16, in which wind loads are simulated by equivalent concentrated loads at every beam-column joint in the *Y*-direction. The total number of random variable is therefore equal to 15. The information of random variables is given in Table 12.

Table 13 shows the comparison of the optimal results of the proposed method and other algorithms. Again, the average of 246.42 *kN* and standard deviation of 6.21 *kN* of the optimum frame weight by using proposed method 2 are similar to those by using proposed method 1. These results are much better than the average weight of 267.56 *kN*, 261.37 *kN*, and 280.37 *kN* of GA, micro-GA, and PSO, respectively. Proposed method 2 continues showing that it is much faster than other methods since its average computational time of 1.84 h is much smaller than those of 32.58, 31.73, 35.47, and 34.66 h of GA, micro-GA, PSO, and proposed method 1, respectively. Therefore, it can be concluded that proposed method 2 is the most effective algorithm in all considered methods. Furthermore, Fig. 17 presents the convergence histories of the best optimum designs of the frame.

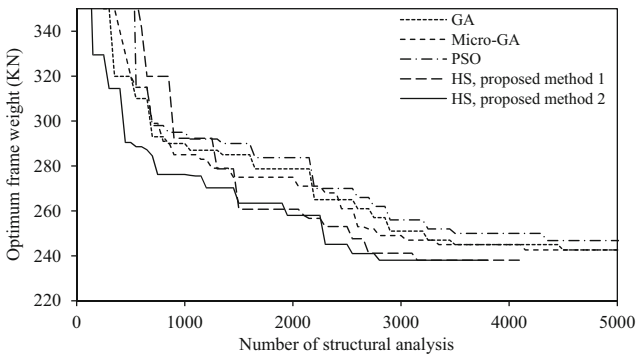

Fig. 17 Convergence histories of the best designs of six-story space frame

8 Conclusion

The summaries and conclusions of this study can be drawn as follows:

(a) An efficient numerical procedure for RBDO of nonlinear inelastic steel space frames is developed by combining the practical advanced analysis, a new robust method of failure probability analysis, and harmony search technique (HS).
(b) The proposed method (IHS-EIS) for evaluating the failure probability of structures is developed by integrating the improved Latin Hypercube (IHS) and a new effective importance sampling (EIS).
(c) The detail implement of HS for discrete optimization of steel frames is introduced.
(d) Compared to Monte Carlo simulation, importance sampling technique (IS), the combination of IS and IHS, and Subset simulation technique, IHS-EIS is much more effective since it requires a smaller number of samples and reduces the computational cost by applying parallel computing.
(e) The proposed implement of HS is shown to be robust in deterministic optimization of steel frames when compared to other metaheuristic algorithms e.g. genetic algorithm, particle swarm optimization, ant colony optimization, Tabu search, etc.
(f) The results of deterministic optimization of the case studies prove that using nonlinear inelastic analysis is preferable to optimization of steel frames.

(g) The proposed procedure for RBDO of steel frames is more stable and effective in the case studies when compared to the genetic algorithm, micro-genetic algorithm, and particle swarm optimization.
(h) The computational time of 0.69 and 1.84 h in RBDO of the two- and six-story space steel frames of the proposed procedure, respectively, proves that this method can be applied in practical design.

Acknowledgements This work was supported by the National Research Foundation of Korea (NRF) grant funded by the Korean government (MSIP) (No.2011-0030040) and (No. 2015R1A2A2A01007339).

References

AISC-LRFD (1999) Manual of steel construction – load and resistance factor design. American Institute of Steel Construction, Chicago

Alberdi R, Khandelwal K (2015) Comparison of robustness of metaheuristic algorithms for steel frame optimization. Eng Struct 102:40–60

Balling R (1991) Optimal steel frame design by simulated annealing. J Struct Eng 117:1780–1795

Bartlett FM, Dexter RJ, Graeser MD, Jelinek JJ, Schmidt BJ, Galambos TV (2003) Updating standard shape material properties database for design and reliability. Eng J AISC 40(1):2–14

Beachkofski BK, Grandhi RV (2002). Improved distributed Hypercube sampling. In 43rd AIAA/ASME/ASCE/AHS/ASC Structures, Structural Dynamics, and Materials Conference, Denver, CO

Bland JA (1995) Discrete-variable optimal structural design using tabu search. Struct Optim 10:87–93

Camp C, Bichon B, Stovall S (2005) Design of steel frames using ant colony optimization. J Struct Eng 131:369–379

Carroll DL (2001) FORTRAN genetic algorithm (GA) driver v1.7.1 [Online], available http://www.cuaerospace.com/carroll/ga.html

Chen WF, Kim SE (1997) LRFD steel design using advanced analysis. CRC Press, Boca Raton

Chen WF, Lui EM (1987) Structural stability: theory and implementation. Elsevier, Amsterdam

Chen WF, Lui EM (1992) Stability design of steel frames. CRC Press, Boca Raton

Clarke MJ (1994) Plastic-zone analysis of frames. In: Chen WF, Toma S (eds) Advanced analysis of steel frames. CRC Press, Boca Raton

Degertekin SO (2007) A comparison of simulated annealing and genetic algorithm for optimum design of nonlinear steel space frames. Struct Multidiscip Optim 34:347–359

Degertekin SO (2008) Optimum design of steel frames using harmony search algorithm. Struct Multidiscip Optim 36:393–401

Degertekin SO, Hayaliolu MS (2010) Harmony search algorithm for minimum cost design of steel frames with semi-rigid connections and column bases. Struct Multidiscip Optim 42:755–768

Doğan E, Saka MP (2012) Optimum design of unbraced steel frames to LRFD–AISC using particle swarm optimization. Adv Eng Softw 46:27–34

Ellingwood BR, MacGregor JG, Galambos TV, Cornell CA (1982) Probability based load criteria: load factors and load combinations. J Struct Div ASCE 108(5):978–997

Engelund S, Rackwitz R (1993) A benchmark study on importance sampling techniques in structural reliability. Struct Saf 12:255–276

Geem ZW, Kim JH, Logonathan GV (2001) A new Heuristic optimization algorithm: harmony search. Simulation 78:60–68

Hasançebi O, Çarbaş S, Doğan E, Erdal F, Saka MP (2009) Performance evaluation of metaheuristic search techniques in the optimum design of real size pin jointed structures. Comput Struct 87(5–6):284–302

Hasançebi O, Çarbaş S, Doğan E, Erdal F, Saka MP (2010a) Comparison of non-deterministic search techniques in the optimum design of real size steel frames. Comput Struct 88(17–18):1033–1048

Hasançebi O, Erdal F, Saka MP (2010b) An adaptive harmony search method for structural optimization. J Struct Eng ASCE 136(4):419–431

Kameshki ES, Saka MP (2003) Genetic algorithm based optimum design of nonlinear steel frames with various semi-rigid connections. J Constr Steel Res 59(1):109–134

Kim SE, Chen WF (1996) Practical advanced analysis for braced steel frame design. J Struct Eng 122:1266–1274

Kripakaran P, Hall B, Gupta A (2011) A genetic algorithm for design of moment-resisting steel frame. Struct Multidiscip Optim 44:559–574

Lee KS, Geem ZW (2004) A new structural optimization method based on the harmony search algorithm. Comput Struct 82:781–798

Li HS, Cao ZJ (2016) Matlab codes of subset simulation for reliability analysis and structural optimization. Struct Multidiscip Optim 54(2): 391–410

Morris MD, Mitchell TJ (1995) Exploratory designs for computer experiments. J Statist Plann Inference 43:381–402

Murren P, Khandelwal K (2014) Design-driven harmony search (DDHS) in steel frame optimization. Eng Struct 59:798–808

Orbison JG, McGuire W, Abel JF (1982) Yield surface applications in nonlinear steel frame analysis. Comput Methods Appl Mech Eng 33(1):557–573

Owen A (1994) Controlling correlations in Latin hypercube samples. J Am Stat Assoc 89:1517–1522

Perez RE, Behdinan K (2007) Particle swarm approach for structural design optimization. Comput Struct 85:1579–1588

Pezeshk S, Camp CV, Chen D (2000) Design of nonlinear framed structures using genetic algorithms. J Struct Eng ASCE 126(3):382–388

Rajeev S, Krishnamoorthy C (1992) Discrete optimization of structures using genetic algorithms. J Struct Eng 118:1233–1250

Saka MP, Geem ZW (2013) Mathematical and metaheuristic applications in design optimization of steel frame structures: an extensive review. Math Probl Eng 2013:1–33

Saka MP, Kameshki E (1998) Optimum design of unbraced rigid frames. Comput Struct 69:433–442

Shayanfar M, Abbasnia R, Khodam A (2014) Development of a GA-based method for reliability-based optimization of structures with discrete and continuous design variables using OpenSees and Tcl. Finite Elem Anal Des 90:61–73

Tada T (2007) FORTRAN particle swarm optimization (PSO) [Online], available http://www.nda.ac.jp/cc/users/tada/

Tang B (1998) Selecting Latin hypercubes using correlation criteria. Stat Sinica 8:965–978

Teh LH, Clarke MJ (1999) Plastic-zone analysis of 3D steel frames using beam elements. J Struct Eng 125:1328–1337

Thai HT, Kim SE (2009) Practical advanced analysis software for nonlinear inelastic analysis of space steel structures. Adv Eng Software 40:786–797

Truong VH, Nguyen PC, Kim SE (2017) An efficient method for optimizing space steel frames with semi-rigid joints using practical advanced analysis and the micro-genetic algorithm. J Constr Steel Res 125:416–427

Tsompanakis Y, Papadrakakis M (2004) Large-scale reliability-based structural optimization. Struct Multidiscip Optim 26:429–440

Valdebenito MA, Schuëller GI (2010) Reliability-based optimization considering design variables of discrete size. Eng Struct 32:2919–2930

Yang YB, Shieh MS (1990) Solution method for nonlinear problems with multiple critical points. AIAA J 28(12):2110–2116

Ye KQ, Li W, Sudjianto A (2000) Algorithmic construction of optimal symmertric Latin hypercube designs. J Statist Plann Inference 90: 145–159